JOURNAL OF MATERIALS SCIENCE 29 (1994) 5327–5332

Natural formation of a protective layer on copper and copper brazing in domestic water: Structural characterization and electrochemical behaviour

H. IDRISSI, J. P. MILLET, S. AUDISIO
Laboratoire de Physicochimie Industrielle INSA de Lyon, F 69621 Villeurbanne Cedex, France
A. IRHZO
Laboratoire d'Electrochimie Faculté des Sciences I Casablanca, Morocco

The coupling Cu/Cu–P brazing, which is that most employed in domestic water supply pipes, has been investigated. Potentiostatic corrosion experiments were performed in domestic water under different conditions. It appears that the brazing has a better resistance than copper. The nature of the films formed at the sample surfaces was determined by various analysis techniques and the thicknesses were measured by ellipsometry. It was observed that it was the difference in composition of the films, formed at copper and brazing surfaces, which allowed the Cu–P brazing to become more noble than copper. The relatively thicker film formed on brazing, appears to contain mainly calcium carbonate and sulphate which grow epitaxially on calcium phosphate (hydroxyapatite or brishite). The corrosion resistance of the studied brazing was not only related to the galvanic coupling copper/brazing, but also depended on other parameters, mainly the water-flow velocity.

1. Introduction

The corrosion of copper in water has been extensively studied by various authors [1–6]. However, little work has been carried out on the behaviour of the materials used for copper brazing [7–10]. In the present work, resistance to corrosion of phosphorous brazings (those most commonly used in the building trade) and their behaviour when coupled to copper, have been studied using electrochemical techniques. The metal was put into a corrosive environment for long periods, and the evolution of the corrosion potential versus time at different flow velocities, as well as diagrams of the electrochemical impedance, have been determined.

In other respects, the nature and composition of the passive films formed have been determined using several analysis techniques (ellipsometry, low-analysis X-ray diffraction, secondary ion mass spectrometry (SIMS), and Raman spectrometry).

Finally, the onset of copper corrosion, due to the formation of a better quality film on the brazing, which thus gives it a more noble behaviour, is discussed.

2. Experimental procedure

The samples tested were de-oxidized copper annealed at 900 °C for 5 min, and phosphorous brazing (7.5 wt % P, 92.5 wt % Cu), the structure of which is $\alpha + Cu_3P$ as shown by a metallographic study (Fig. 1). This brazing was melted in order to produce a cylindrical-shaped piece (diameter 7 mm and length 15 mm). This was then coated with Teflon, so that only a plane section of 0.38 cm^2 was in contact with the medium of study, in this case, Villeurbanne water (domestic water), the composition and characteristics of which are given in Tables I and II.

The electrochemical equipment, used to record the natural corrosion potential evolution and the electrochemical impedance diagrams, consisted in a Schlumberger apparatus (potentiostat type 1286, frequency response analyser type 1250) conducted by a microcomputer Apple IIe. The electrochemical cell was a Pyrex double-walled one. Its lid was equipped with conical grindings that allowed the fixing of the electrodes (working, saturated calomel reference, ECS, and counter electrodes). The working electrode was adapted to an EDI Tacussel rotating device, the speed of which was set at between 0 and 1000 r.p.m. The cell and its lid were coated with an opaque black paint in order to prevent all penetration of light which could modify the interactions at the metal/solution interface.

The influence of the flow velocity on corrosion potential was studied on a sample that had been previously polished, cleaned with alcohol, dried in an azote stream, and immersed in water at 20 °C for up to 10 h. Then the sample was then subjected to rotation.

The impedance tests were carried out at room temperature and the diagrams were obtained at the free corrosion potential. The amplitude of the applied sinusoidal perturbation was ± 5 mV, the frequency

0022–2461

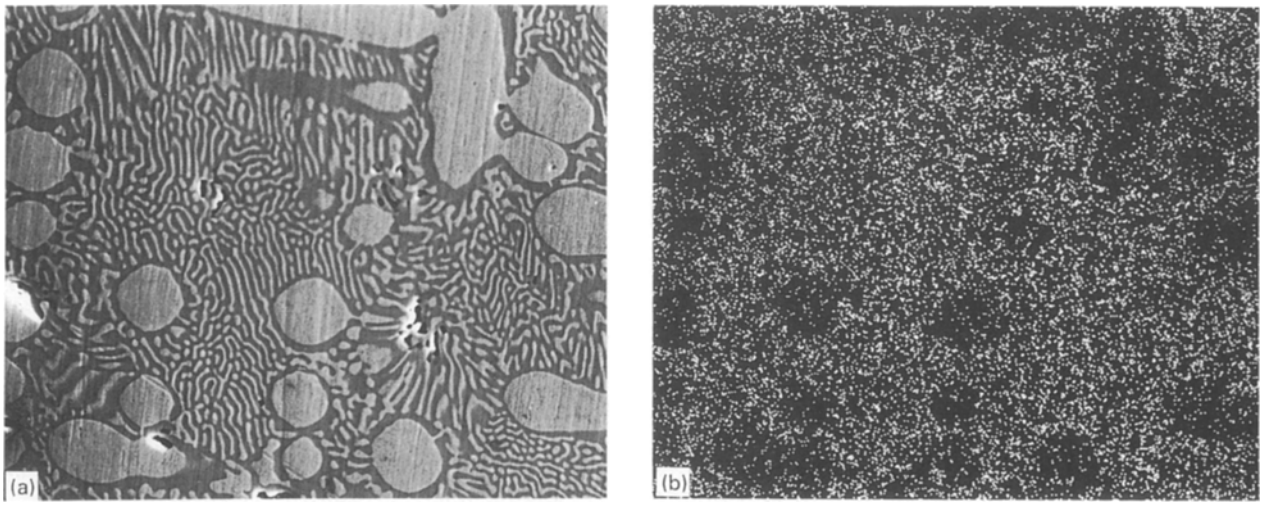

Figure 1(a) Metallographic structure of the brazing obtained by MEB. (b) X-image of elemental phosphorus in the brazing.

TABLE I Chemical composition (mg l^{-1}) of the testing water

Ca^{2+}	Mg^{2+}	Na^{+}	K^{+}	CO_3^{2-}	HCO_3^{-}	SO_4^{2-}	Cl^{-}	NO_3^{-}	Diss. sol.
72.6	6.43	4.14	1.95	0.15	212	24	7.81	4.34	259

TABLE II Characteristics of the testing water

T (°C)	pH	TH as $CaCO_3$ ($mg l^{-1}$)	TAC as $CaCO_3$ ($mg l^{-1}$)	Resistivity ($\Omega\ cm^{-1}$)
20	7.35	196	169	2780

scan was from 10^5 to 10^{-2} Hz and the integration was made on five points per decade.

The ellipsometric measurements were performed using a spectroellipsometer of the revolving analyser type, allowing the sample evolution to be followed *in situ* in its surrounding. These *in situ* measurements were conducted at a wavelength of $\lambda = 633$ nm.

3. Results

Fig. 1a shows the metallographic structure obtained by MEB. Copper nodules, corresponding to the α phase, as seen to be swamped by a lamellar structure, Cu_3P. Fig. 1b shows the distribution of elemental phosphorus in the brazing Cu–P. The low concentration of this element in copper nodules is clearly apparent.

Figs 2–4 show examples of curves obtained from the electrochemical tests and ellipsometric *in situ* analysis. Fig. 2 shows, for the two materials, the evolution of the corrosion potential versus time at 20 °C. The curves obtained do not have the same aspect. For copper, the corrosion potential increases with time and then remains almost stable after about 30 min. For the brazing, the potential decreases initially, and then increases towards a more positive potential, before reaching a level value. It can be noticed in this figure that E_{cor} values, after about 2 h immersion, are higher for the brazing than for copper.

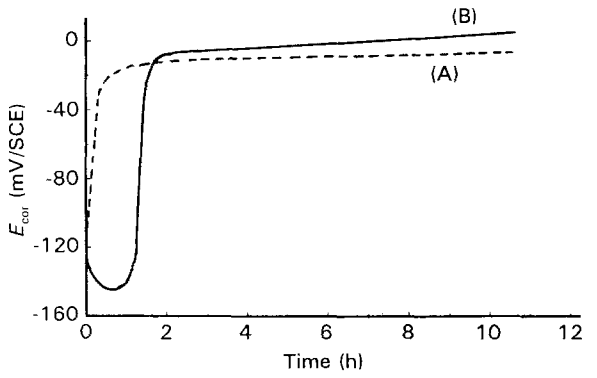

Figure 2 Open circuit potential versus time curves in cold water (20 °C). (A) Copper, (B) Cu–P brazing.

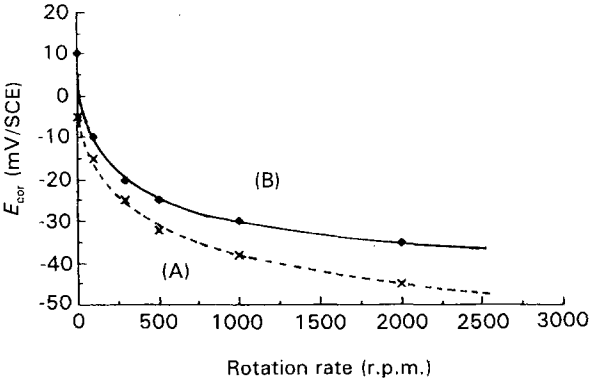

Figure 3 Potential–flow velocity curves of (A) copper and (B) Cu–P brazing in the tested water.

Fig. 3 shows the influence of water-flow velocity on the corrosion potential. The values are those read after the sample had been kept for 15 h in stagnant water at 20 °C. Increasing flow velocity leads to a decrease of the corrosion potential for both brazing and copper.

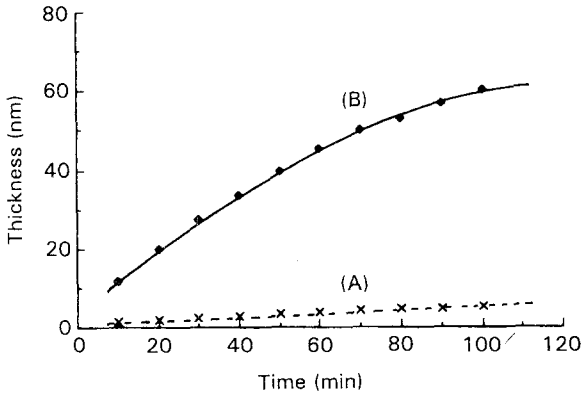

Figure 4 Film thickness formed on (A) copper and (B) Cu-P brazing versus time of immersion in cold water (20 °C).

TABLE III Refractive indices of the substrates and films formed on copper and brazing

Samples	substracte index, n_1	film index, n_2
Copper	0.33	2.00
Brazing	2.13	2.04

Curves obtained by *in situ* ellipsometric analysis, showing the growth of films formed at copper and brazing surfaces, are given in Fig. 4. It is noticed that after immersion of the samples in water, the film formed on the brazing (curve B) increases much more rapidly than that formed on copper (curve A). The refractive indices of the substrates and films are given in Table III.

Fig. 5 gives the electrochemical impedance diagrams of copper and brazing obtained after various immersion times (5 min, 2 and 10 h) at the natural potential of corrosion. These diagrams show the existence of two loops, which are even more pronounced when the immersion time of the samples is increased. Table IV collated the characteristic values of film capacity, C_f, film resistance, R_f, Helmoltz double layer capacity, C_d, and the transfer charge resistance, R_t, read from these diagrams.

The concentration profile, obtained by SIMS, of the elements present in the film formed on copper and brazing after 2 h immersion is given in Fig. 6. The main results of the analysis carried out on these films using several techniques (X-ray diffraction, Raman spectrometry) are given in Table V. So, the film form-

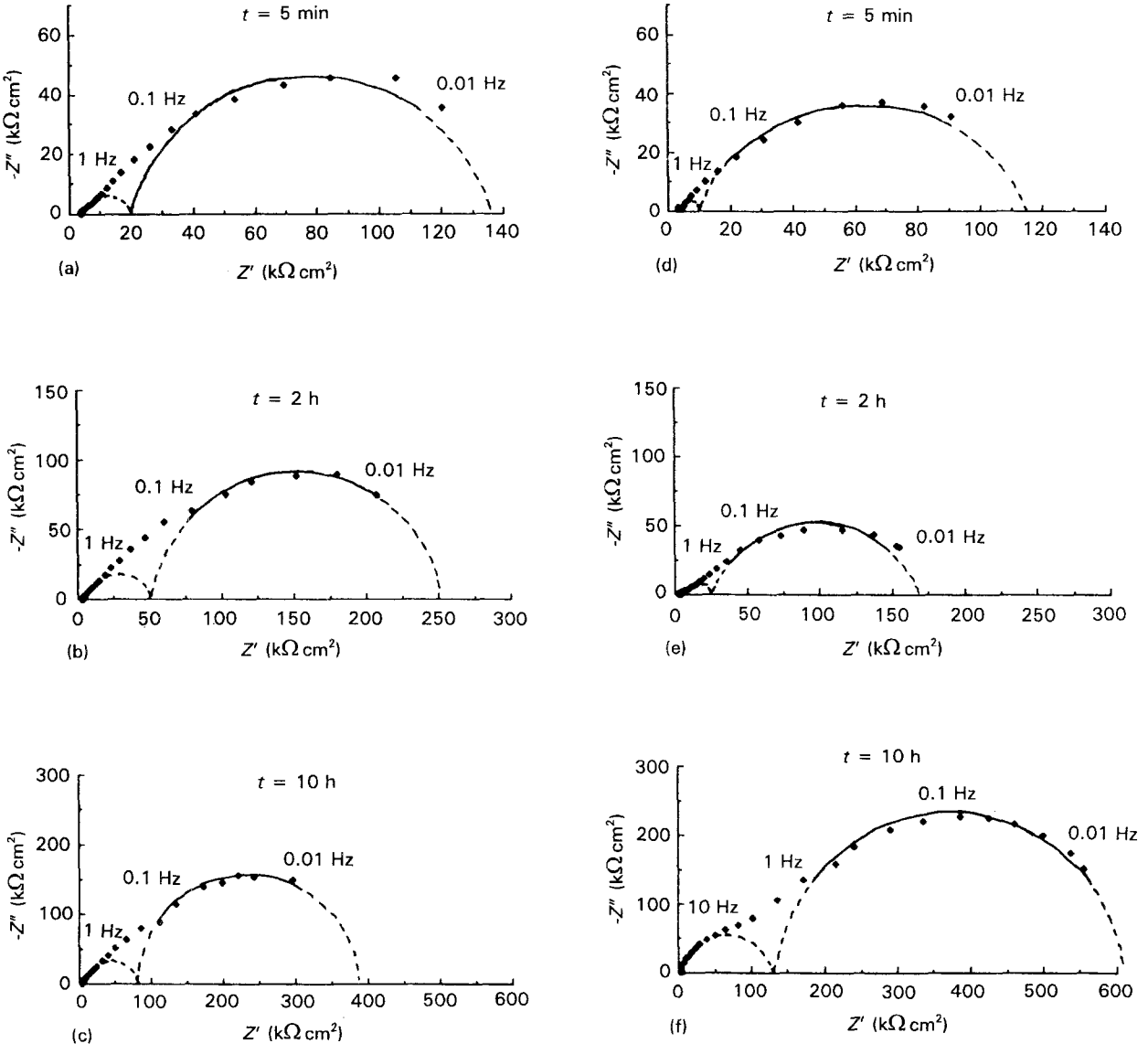

Figure 5 Electrochemical impedance diagrams at different immersion times. (a–c) Copper, (d–f) Cu–P brazing.

TABLE IV Characteristic values obtained from impedance diagrams of copper (A) and Cu-P brazing (B)

	Copper			Brazing		
	5 min	2 h	10 h	5 min	2 h	10 h
$C_f(\mu F\,cm^{-2})$	–	3.2	2.1	–	1.1	0.3
R_f ($k\Omega\,cm^2$)	–	48.7	76.3	–	22.3	127.6
$C_d(\mu F\,cm^{-2})$	48.5	31.6	19.6	36.2	21.1	8.4
R_t ($k\Omega\,cm^2$)	130.5	200	313	110.5	146	473.6

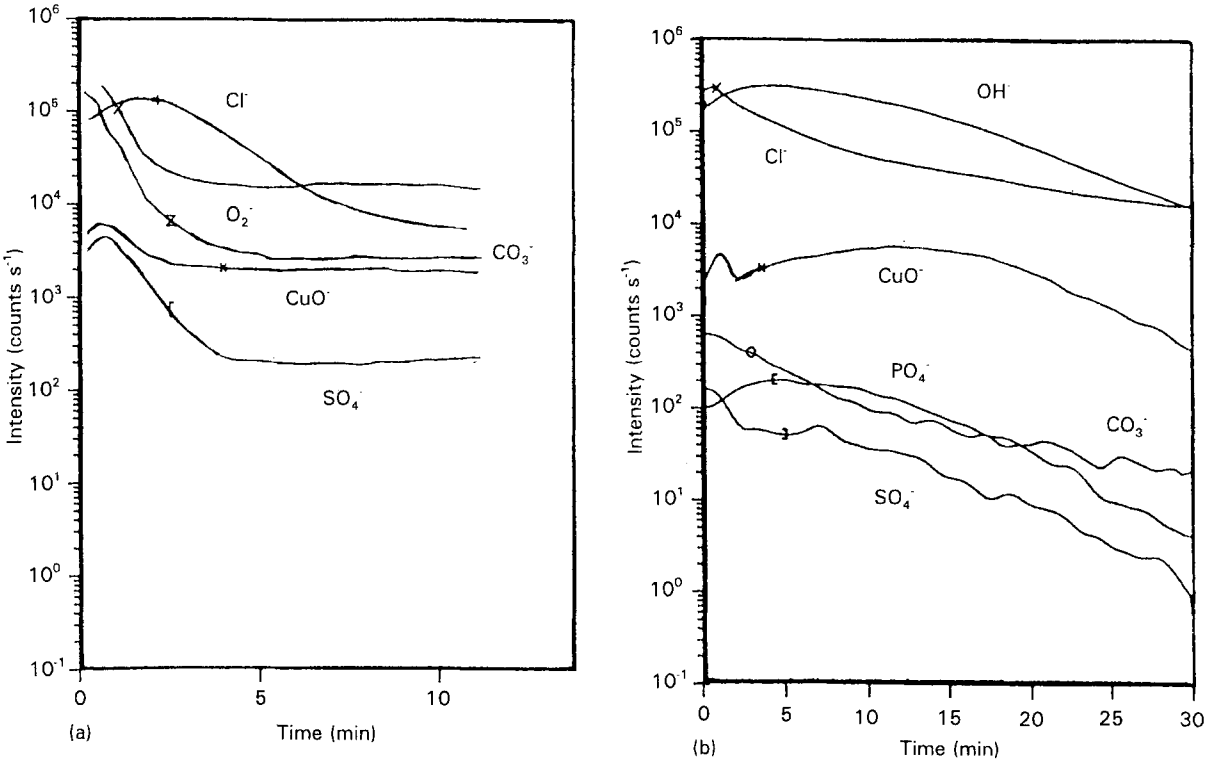

Figure 6 Concentration profiles obtained by SIMS on (a) copper and (b) Cu–P brazing films, after 2 h immersion.

TABLE V Composition analysis of films formed on copper (A) and Cu-P brazing (B) (X-ray diffraction, Raman scattering).

	Substrate	
Technique	A	B copper Cu–P brazing
X-ray	Cu_2O	$Ca\,CO_3$
		Cu_2O
Raman	SO_4^{2-}	SO_4^{2-}
	CO_3^{2-}	CO_3^{2-}
	Cu–O	Cu–O

ed on copper is mainly made of cuprous oxide, calcium sulphate and traces of carbonate, while the film formed on the brazing is mainly constituted by cuprous oxide and calcium carbonate [10].

4. Discussion

The corrosion potential versus time curves show that, for copper, E_{cor} increases just after immersion, whereas, for brazing, a decrease in E_{cor} is first noticed, followed by a rapid increase. The Nyquist diagrams obtained for the two materials indicate the electrochemical charge during the immersion time. This is characterized by the existence of two capacitive semicircles. The parameters of the first one, C_f and R_f, characteristic of the films formed at the sample surface, are measured in the high-frequency field. On another hand, parameters of the second semicircle, C_d and R_t, correspond to the electrochemical reactions of the inner Helmoltz double layer and transfer charge resistance. In this case, the capacity, C_d, and resistance, R_t were obtained at low frequency. Examination of these diagrams reveals that the resistances at low frequency, R_t, increase quicker during the immersion time for brazing than for copper (high electrochemical barrier) exhibiting even a decrease of the surface on which the electrochemical processes can act. This difference in behaviour seems to be linked to the composition of the brazing. Similarly, if the resistance, R_f, at high frequency, is considered, a larger increase for brazing is noted. Such an increase is due to the coating of the electrode surface with a film which forms a barrier layer, slowing down metal dissolution. This interpretation is in good agreement with that given by Keddam [12] on the study of the protective paint film realized on steel.

The ellipsometric study shows that the film formed

on brazing grows more rapidly than that formed on copper, and it is thicker, which leads to a better corrosion resistance. This can be explained by considering the composition of the brazing $Cu_3P + \alpha$. Indeed, during immersion of this brazing in water, the compound Cu_3P is attacked by dissolved oxygen (O_2) and by oxides Cu_2O and CuO formed during oxidation of the α-phase, giving orthophosphoric acid, H_3PO_4, according to the reactions [7]

$$3Cu + (O_2)_{dis} \rightarrow Cu_2O + CuO \quad (1)$$

$$2Cu_3P + 5/2O_2 + 3H_2O \rightarrow 2H_3PO_4 + 6Cu \quad (2)$$

$$2Cu_3P + 5CuO + 3H_2O \rightarrow 2H_3PO_4 + 11Cu \quad (3)$$

$$2Cu_3P + 5Cu_2O + 3H_2O \rightarrow 2H_3PO_4 + 16Cu \quad (4)$$

Because the pH of the medium (Villeurbanne water) is close to 7, orthophosphoric acid dissociates according to the reactions

$$H_2O + H_3PO_4 \rightarrow H_2PO_4^- + H_3O^+ \quad (5)$$

$$H_2O + H_2PO_4^- \rightarrow HPO_4^{2-} + H_3O^+ \quad (6)$$

$$H_2O + HPO_4^{2-} \rightarrow PO_4^{3-} + H_3O^+ \quad (7)$$

PO_4^{3-} and HPO_4^{2-} ions, which are very active, react with ions coming from dissolved salts in the water to form calcium phosphate $Ca_5(PO_4)_3(OH)$ (hydroxyapatite) and $CaHPO_4 \cdot 2H_2O$ (brishite). These phosphates are insoluble and remain at the brazing surface. These products quickly form a protective layer: the corrosion current decreases and the transfer resistance R_t increases. The more insulating is this layer, the higher will be the transfer resistance. Therefore, it appears, after the first hour of immersion, that the film formed at the brazing surface is more protective than that formed on copper. SIMS analysis shows that the concentration profile of Cl^- increases initially from the copper substrate, reaching maximum in the film and then decreasing from the film towards the film/water interface. In the same way, this analysis shows that the concentration of CuO, CO_3^{2-}, SO_4^{2-} present in the layer formed on the brazing is almost twice that present in the film formed on copper. This difference in nature and thickness of the film is emphasized when the flow velocity increases, thus leading to the evolution of the corrosion potential mentioned in Fig. 3.

Examination of the structure of $CaCO_3$, $CaSO_4$, $Ca_5(PO_4)_3(OH)$, and $CaHPO_4 \cdot 2H_2O$ compounds [13–15] shows, moreover, that the high atomic density plan of the structure $Ca_5(PO_4)_3(OH)$ (hydroxyapatite) is a multiple plan of its homologue existing in the $CaCO_3$ (calcite) structure, which leads to epitaxial growth.

Simultaneous to this growth, SO_4^{2-} ions from dissolved salts replace the HPO_4^{2-} ions of the $CaHPO_4 \cdot 2H_2O$ phosphate formed during the brazing attack. This substitution leads to the formation of $CaSO_4 \cdot 2H_2O$ sulphate, the structure of which is a perfect isotype of that of $CaHPO_4 \cdot 2H_2O$ phosphate.

This $CaSO_4 \cdot 2H_2O$ sulphate can also grow in an epitaxial manner on the $CaHPO_4 \cdot 2H_2O$ structure, because of the isotypy of both structures, as demonstrated by several authors [14, 15]. The formation, at the brazing surface, of these passive films with a thickness and quality superior to those formed on the copper surface, allows improvement of its corrosion resistance. At the time of its coupling with copper, this brazing is less noble and anodic reactions are favoured on the surface, close to the brazing, whereas cathodic reactions are favoured on the brazing.

This copper/brazing galvanic corrosion [8] is activated by an increase in the flow velocity (Fig. 3). On the brazing area, copper corrodes and progressively disappears. Thus, corrosion–erosion of copper can be developed at high flow velocities and copper is then, locally, laid bare. Under these conditions, the passive copper/brazing coupling gives way, on the one hand, to the bare copper/brazing coupling (much more unfavourable), and, on the other hand, to the bare copper/passive copper coupling. This latter coupling is also very unfavourable, because the anode/cathode area ratio is less than 1. The simultaneous action of these three corrosion phenomena, galvanic copper/brazing coupling, corrosion/erosion and galvanic bare copper/passive copper coupling, leads to the rapid and local perforation of the copper.

5. Conclusion

The electrochemical study has ascertained that, when copper and brazing are left in water, the formation of less or more passive films occurs, the film formed on the brazing being more resistant than that formed on copper. An increase in flow velocity leads to destruction of these films, according to their nature.

Surface analysis results indicate that the film formed in cold water on copper, is mainly constituted of cuprous oxide with chloride and calcium carbonate traces. The film formed on the brazing essentially consists of cuprous oxide and large quantities of calcium carbonate and calcium sulphate. This study reveals that, at the time of copper/brazing coupling, the brazing is more noble than the copper. The relative higher nobleness, linked to the formation of a protective, more insulated, film on the brazing than on the copper, favours a cathodic reaction on the brazing. The more protective natural film on the brazing becomes more efficient due to the epitaxial growth of calcium carbonate and products linked to the cathodic reactions.

References

1. M. F. OBRECHT, *Corrosion* **18** (1962) 189.
2. V. F. LUCEY, *Br. Corr. J.* **2** (1967) 176.
3. M. POURBAIX, J. VAN MUYLDER and P. VAN LAER, *Corr. Sci.* **7** (1967) 795.
4. E. MATTSSON and A. M. FREDRIKSSON, *Br. Corr. J.* **3** (1968) 246.
5. L. KNUTSSON, E. MATTSSON and B. E. RAMBERG, *ibid.* **7** (1972) 208.
6. F. J. CORNWEL, G. WILSMITH and P. T. GILBERT, *ibid.* **8** (1973) 202.
7. O. WOLLRAB, *Schadenprisma* **4** (1983) 50.
8. H. IDRISSI, 87 ISAL 0045, Lyon (1987).
9. H. IDRISSI, S. AUDISIO, A. ELMOUAFFEK and M. CHASTRETTE, *Matériaux et Techniques*, **75** (10, 11) (1987) 433.

10. H. IDRISSI, J. C. DUPUY, J. C. BUREAU and S. AUDISIO, in "Proceedings of the 6th International Conference on Secondary Ion Mass Spectroscopy", Versailles, 13–18 September 1987, edited by A. Benninghoven, A. M. Huber and H. W. Werner (Wiley, New York, 1987), pp. 1003–6.
11. A. IRHZO, M. EL SAFTY, N. BUI and F. DABOSI, in "Proceedings of the 10th International Congress on Metallic Corrosion", Madras, 7–11 November 1987, edited by K. I. Vasu (Oxford and IBH publishing Co, Pvt Ltd, New Delhi) pp. 3953–60.
12. M. KEDDAM, in Journée CEFRACOR: "L'électrochimie, des outils contre la corrosion", Montrouge, November 1992, Proceedings, pp. 3953–60.
13. H. IDRISSI, S. AUDISIO and A. GAGNAIRE, *Matériaux et Techniques*, **78** (1, 2) (1990) 29.
14. M. MURAT, in "Proceedings of the RILEM International Symposium", Saint Rémy lès Cheureuses, Paris, May 1977, edited by M. Murat and M. Foucault (Paris, 1977).
15. E. E. BERRY, *J. Appl. Chem. Biotechnol.* **22** (1972) 667.

Received 17 January
and accepted 13 April 1994